

Vol. 1, Part 1, p. 343.

⁶J. Yamashita and K. Inoue, *J. Phys. Chem. Solids* **12**, 1 (1959); N. I. Meyer and M. H. Jørgensen, *ibid.* **26**, 823 (1965).

⁷H. G. Reik and H. Risken, *Phys. Rev.* **126**, 1737 (1962).

⁸W. P. Dumke, *Phys. Rev. B* **2**, 987 (1970).

⁹W. Fawcett and E. G. S. Paige, *Electron. Letters* **3**, 505 (1967).

¹⁰E. M. Conwell, *High-Field Transport in Semiconductors* (Academic, New York, 1967).

¹¹W. Fawcett and E. G. S. Paige (private communication).

¹²H. J. G. Meyer, *Phys. Rev.* **112**, 298 (1958); *J. Phys. Chem. Solids* **8**, 264 (1959).

¹³M. Lax and R. Rosenberg, *Phys. Rev.* **112**, 843 (1958).

¹⁴S. M. deVeer and H. J. G. Meyer, in *Proceedings of the International Conference on the Physics of Semiconductors, Exeter, England, 1962* (The Institute of Physics and the Physical Society, London, 1962), p. 358.

¹⁵E. G. S. Paige, *Progress in Semiconductors* (Heywood, London, 1964), Vol. 8, pp. 105, 106.

¹⁶B. R. Nag and H. Paria, *J. Appl. Phys.* **37**, 2319 (1966).

¹⁷M. H. Jørgensen, N. I. Meyer, and K. J. Schmidt-Tiedemann, in *Proceedings of the Seventh International Conference on the Physics of Semiconductors, Paris, France, 1964* (Academic, New York, 1964), p. 457.

Magnetic Freezeout and Impact Ionization in GaAs[†]

T. O. Poehler

Applied Physics Laboratory, The Johns Hopkins University, Silver Spring, Maryland 20910

(Received 17 March 1971)

Low-temperature measurements of impurity effects have been conducted in n -type GaAs with impurity concentrations of the order of $(1-3) \times 10^{15} \text{ cm}^{-3}$. The behavior of these materials in strong magnetic fields is well described by a recently developed theory which characterizes the impurity level with a broadened energy distribution and the conduction band with a Gaussian-like tail. The reduced impurity ionization energies in strongly doped materials are explained in terms of this model. Electric field ionization of these impurity levels in strong magnetic fields was found to be consistent with the model and recent theories of impact-ionization phenomena.

INTRODUCTION

Recent work on epitaxial growth of n -type GaAs films has yielded samples with electron concentrations as low as $1 \times 10^{12} \text{ cm}^{-3}$ and a well-defined impurity level separated from the conduction-band edge by approximately 0.005 eV.¹⁻³ In studies of far-infrared photoconductivity and cyclotron resonance in this material, samples with donor impurity concentrations on the order of $1 \times 10^{15} \text{ cm}^{-3}$ have proven to be widely used. For GaAs with impurity concentrations in this range, the electron concentration in the conduction band depends on the temperature and magnetic field strength in a manner similar to that previously described for InSb⁴ and InAs.⁵

At low temperature, some electrons in GaAs are frozen out of the conduction band into impurity bound states. However, in the absence of a magnetic field, an appreciable fraction of the carriers remain free in the conduction band. These free carriers are the result of a reduced donor activation energy in strongly doped materials caused by tails on the densities of states of the conduction band and impurity level. Application of an intense magnetic field H shrinks the volume

of the electronic wave function to a region less than that occupied by an impurity ion. Charge carriers are frozen out of the lowest-order conduction-band Landau level onto localized states with a binding energy \mathcal{E}_b , which increases with magnetic field. This magnetic freezeout is characterized by an increase in the Hall coefficient with magnetic field at a fixed temperature T .

This paper reports on measurements of the temperature and magnetic field dependence of electron concentration of n -type GaAs in the freezeout regime. The binding energy $\mathcal{E}_b(H)$ has a magnetic field dependence of $\mathcal{E}_b \propto H^{1/3}$ as has been previously observed in n -InSb⁴ and n -InAs.⁵ The magnitude of the binding energy is less than that measured in experiments on lightly doped samples or predicted by theoretical calculations.^{6,7} The results can be explained by resorting to the recently developed model of a strongly doped semiconductor in a magnetic field.⁸ In this model, which is based on spatial fluctuations in a random impurity potential, there is a tail on the conduction-band density of states and a broadened impurity level leading to a temperature- and field-dependent ionization energy. A reasonably accurate picture of the band tailing and impurity

level broadening in GaAs can be determined from a combination of the experimental results and the theoretical model. Further, the reduced activation energy can be explained in terms of the model, as can the extremely small electron mobility at low temperature.

Measurements have also been made on low-temperature electrical breakdown in strong magnetic fields where the shift of the energy levels is significant. The results are interpreted in terms of recent theories of impact ionization^{9,10} of impurity levels taking into account the effects of magnetic field on energy-level separation.

EXPERIMENTAL

The experiments were conducted using *n*-type GaAs epitaxial layers deposited on Cr-doped GaAs substrates with resistivities of $1 \times 10^8 \Omega \text{ cm}$. Most of the measurements reported here were made on samples cut from a wafer with an epitaxial layer with a room-temperature carrier concentration of $2.15 \times 10^{15} \text{ cm}^{-3}$, a compensation ratio of 0.2, mobility of $7 \times 10^3 \text{ cm}^2/\text{V sec}$, and thickness of $100 \mu\text{m}$. Ohmic electrical contacts were made by alloying an evaporated Au-Sn layer with the GaAs at 400°C in a vacuum. Hall-effect measurements were made on samples with large area current contacts while Hall voltages were measured on a set of contacts constructed to allow balancing out of error voltages. A high-impedance dc source was used to supply current to the specimen while voltages were measured using high-input-impedance instruments together with an *x-y* recorder. The measurements at 4.2°K were made in a 60-kOe superconducting magnet while other experiments were conducted

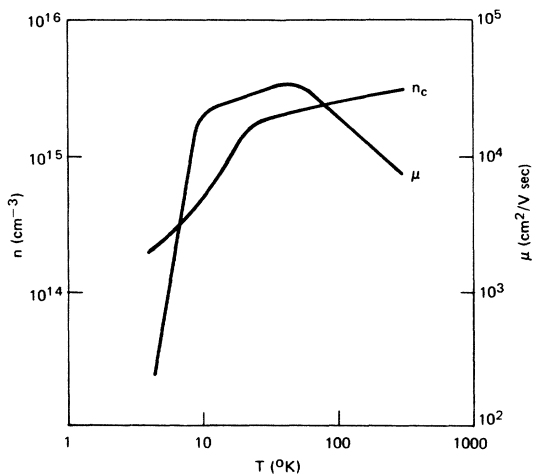


FIG. 1. Temperature dependence of electron concentration and mobility in *n*-type GaAs specimen. Measurements made at magnetic field of 4.5 kOe with electric field strength less than 0.1 V/cm.

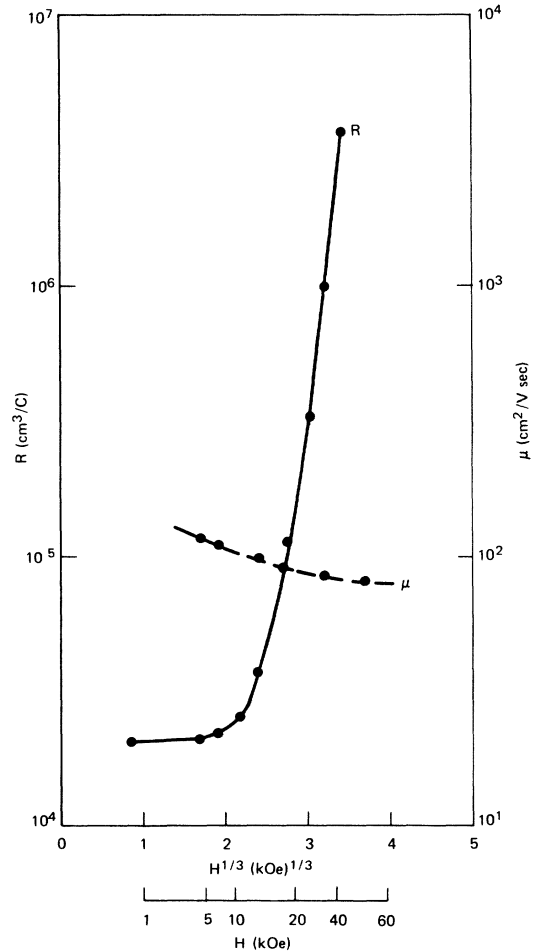


FIG. 2. Magnetic field dependence of the Hall coefficient of *n*-type GaAs specimen with $N_D - N_A = 2 \times 10^{15} \text{ cm}^{-3}$.

in a 20-kOe electromagnet.

The temperature dependence of the electron concentration and the electron mobility in a typical GaAs specimen at low magnetic field strength are shown in Fig. 1. The mobility data show that phonon scattering is dominant at temperatures down to 70°K . Below 70°K ionized impurity scattering is the predominant mechanism, although below about 10°K a sharp reduction in mobility is observed as a result of carriers in localized states. The carrier concentration drops very slowly down to 20°K , then there is a decline of approximately an order of magnitude below 20°K .

At 4.2°K the Hall coefficient and transverse magnetoresistance were measured as a function of magnetic field up to fields of 50 kG. The Hall coefficient for a representative sample is plotted in Fig. 2 showing a magnetic field dependence of $H^{1/3}$ over most of the measured range. In both this data and that related to temperature depen-

dence, the magnitude of the binding energy is considerably smaller than the values based on hydrogenic models.^{6,7} In this freezeout regime, the electron mobility calculated from these measurements was found to decrease slowly with increasing magnetic field, as is also illustrated in Fig. 2.

Measurements were also made of the low-temperature impact ionization of the impurity levels in relatively modest electric fields. At zero magnetic field the current-voltage characteristic consists of an Ohmic region where the current is proportional to the applied electric field strength and a prebreakdown region where the current is a nonlinear function of field strength. At a critical field strength of approximately 7.5 V/cm, breakdown occurs accompanied by a small negative-resistance effect and a transition to a sustaining field strength of 6.3 V/cm (Fig. 3). The low ratio between breakdown and sustaining field strengths is a characteristic of materials which are weakly compensated.

The application of a magnetic field perpendicular to the direction of the electric field causes significant changes to the current-voltage characteristic. In the Ohmic and prebreakdown regions the resistivity increases with field, with the Ohmic region extending to higher electric field strengths in strong magnetic fields. The electric field strength required to induce impact ionization is seen to increase with increasing magnetic fields. The relationship between breakdown field and magnetic field consists of a slowly changing region at low magnetic fields followed by an essentially linear increase in breakdown electric field above 10 kOe. Several samples had a minimum electric breakdown field at magnetic field strengths of approximately 5 kOe as illustrated in Fig. 4. Measurements made on some specimens in longitudinal magnetic fields showed some increase in breakdown electric field strength, but the change was only a small fraction of the variation observed

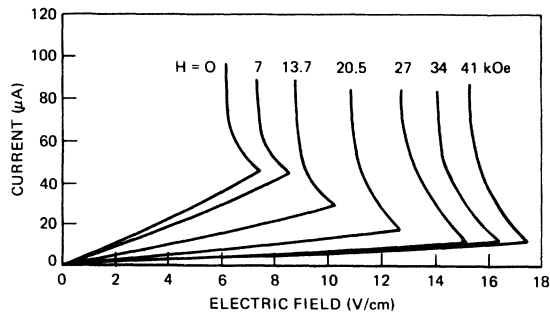


FIG. 3. Current-electric field characteristics for *n*-type GaAs layer at 4.2°K. Characteristic curves are shown for values of magnetic field strength applied normal to direction of electric field.

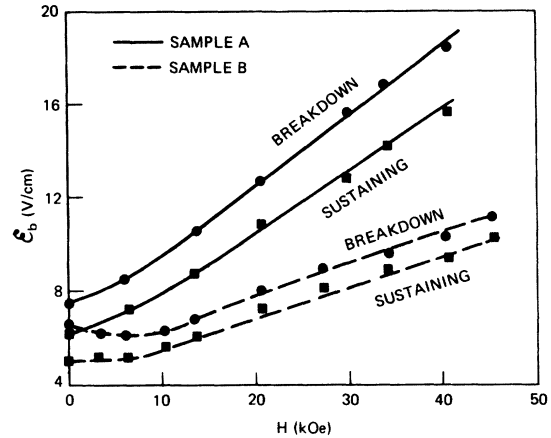


FIG. 4. Breakdown and sustaining electric field strengths in transverse magnetic fields. Sample A: $(N_D - N_A) = 2 \times 10^{15} \text{ cm}^{-3}$, $t = 100 \mu\text{m}$; sample B: $(N_D - N_A) = 1 \times 10^{15} \text{ cm}^{-3}$, $t = 100 \mu\text{m}$.

in a transverse magnetic field as shown in Fig. 4. The results on all the specimens were independent of the field polarities indicating that bulk phenomena were being observed.

Freezeout and Band Tailing

The low-temperature Hall effect, magnetoresistance, and impact-ionization measurements in *n*-type GaAs can be explained in terms of impurity ionization from impurity levels broadened by fluctuation effects. In this model there is a random distribution of ions in the host crystal so that there will exist fluctuations in the spatial density of impurity ions. The spatial density variations cause fluctuations in the potential energy of electrons although within a volume $\frac{4}{3}\pi\lambda_s^3$, where λ_s is the screening length, the potential may be taken as approximately constant. The density-of-states function for the whole crystal can be found by averaging local density functions for each region over a potential distribution. This procedure yields density-of-states functions for the conduction band and impurity level in a magnetic field quite distinct from the usual densities of states in a field. In Fig. 5(a) is shown the density-of-states functions for an impurity level and the lowest-order Landau level of the conduction band in a magnetic field for the case of a lightly doped material. The ionization energy \mathcal{E}_b , predicted by the hydrogenic theory and its dependence on magnetic field are shown in Fig. 6. The ionization energy for the unbroadened densities of states is seen to be 5.2 meV at zero magnetic field increasing to 9.0 meV at 60 kOe. For the more heavily doped specimen where the impurity level and conduction band are broadened with Gaussian profiles, the density-of-states functions appear as pictured in Fig. 5(b). The conduction-

band and impurity densities $\rho_c(x)$ and $\rho_b(x)$, respectively, are given by⁸

$$\rho_c(x) = \frac{eH}{c\hbar^2} \left(\frac{2m^*}{\pi\Gamma} \right)^{1/2} \int_{-\infty}^x dy \frac{e^{-y^2}}{(x-y)^{1/2}}, \quad (1)$$

$$\rho_b(x) = (N_D/\pi^{1/2}\Gamma) e^{-(x+x_b)^2}, \quad (2)$$

where m^* is the electron effective mass and N_D is the donor impurity density. The parameter x is the energy \mathcal{E} normalized to the average value of the fluctuation potential Γ , so that x_b is \mathcal{E}_b/Γ . The fluctuation potential which is a measure of the broadening of densities of states is given by

$$\Gamma = (2e^2/\kappa)(N\pi\lambda_s)^{1/2}, \quad (3)$$

where κ is the static dielectric constant and N is the total impurity concentration.

In this model, the number of carriers n_c in the conduction band of a lightly compensated material can be written as

$$n_c = n_0 \exp[-\mathcal{E}_b/kT + (\Gamma/2kT)^2], \quad (4)$$

where $n_0 = (2\pi)^{1/2} eH(nkT)^{1/2}/h^2c$. From the experimental results in the freezeout regime we may use Eq. (4) to calculate values of Γ . These

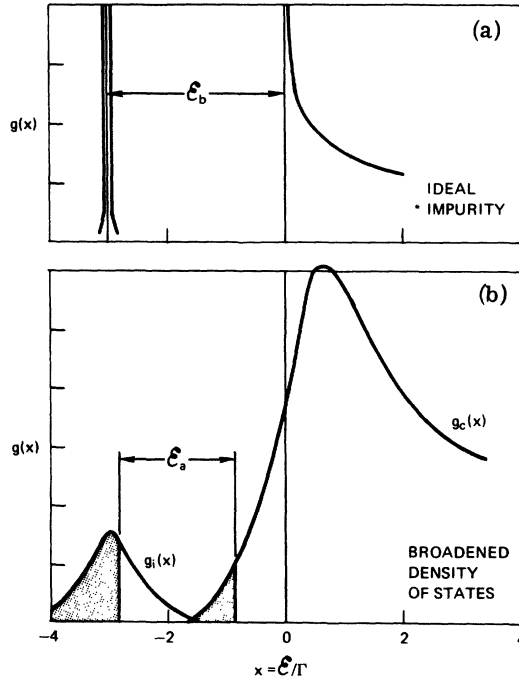


FIG. 5. Density-of-states functions for n -type GaAs in a strong magnetic field. (a) Ideal case of lightly doped specimen with binding energy \mathcal{E}_b . (b) Broadened density-of-states functions in strongly doped material with ionization energy \mathcal{E}_i . Energy normalized by Γ , where $\Gamma \cong 3$ meV at $H = 40$ kOe.

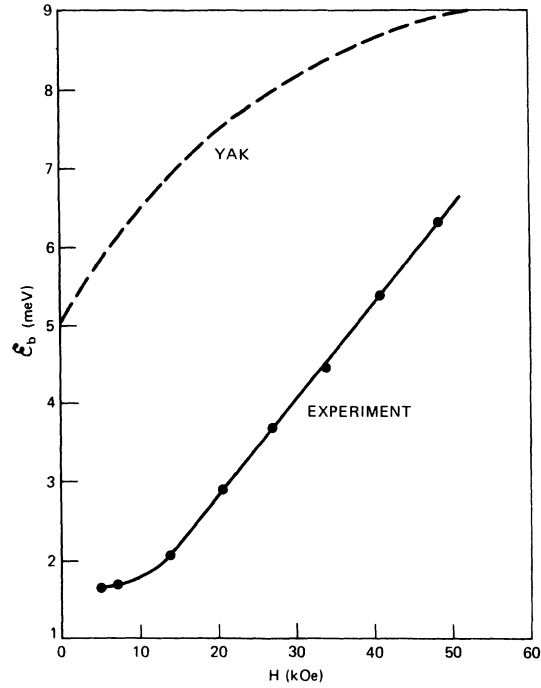


FIG. 6. Theoretical and experimental values of impurity ionization energy in n -type GaAs in a magnetic field.

experimentally derived values for Γ may be compared with theoretical values from Eq. (3) for various values of the magnetic field H . The screening length used in the calculation of Γ is the quantum screening length λ_s , where

$$\lambda_s^2 = n_c^{-1/3} \left(\frac{1}{3}\pi \right)^{1/3} \frac{1}{4} a^* \quad (5)$$

and a^* is the effective Bohr radius of the carriers ($a^* = \kappa\hbar^2/m^*e^2$). The experimental and theoretical values of the fluctuation potential are plotted in Fig. 7 together with the quantum screening radius as a function of magnetic field. Agreement between the experimental and theoretical values of Γ is reasonably good using this screening radius, while the classical radius also pictured in Fig. 7 is seen to vary too rapidly with magnetic field to correspond to the experimental values for Γ .

The results observed in n -type GaAs in the magnetic freezeout regime do appear to be properly characterized by a theory including band tailing and broadening. However, the impurity ionization energies as deduced from the slope of the Hall coefficient as a function of magnetic field strength are only a fraction of those predicted by theory (Fig. 6). Further, the tail of the conduction band and the impurity level have at least some degree of overlap according to these calculations.

The actual ionization energy is measured from

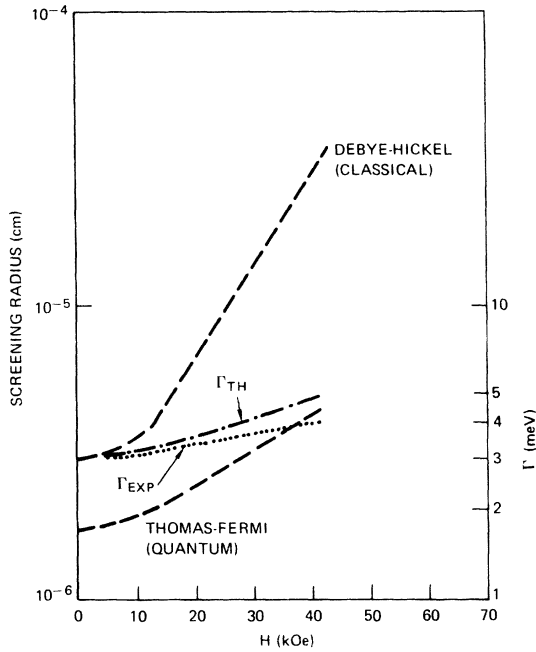


FIG. 7. Experimental and theoretical values of the fluctuational potential Γ as a function of magnetic field. Also shown is the quantum screening radius used to calculate Γ together with the classical screening radius which appears inappropriate to describe this case.

the Fermi level located slightly above the center of the impurity level and a certain critical energy in the conduction band. States at the bottom of the conduction tail are of low density and are sufficiently localized that they do not contribute to the conduction process.¹¹ The criterion proposed by Mott¹¹ is that the localized states occur when the density of states falls to about $\frac{1}{5}$ of the full density, and this is indicated by the shaded portion of Fig. 5. The energy required to excite an electron from an impurity state to a conducting state is seen to be a fraction of the binding energy calculated from the previous descriptions. These magnetic-field-dependent values are more nearly in agreement with the experimentally measured ionization energy.

Impact Ionization

The low-temperature electric breakdown observed in this material is caused by impact ionization of neutral impurity centers by hot carriers.¹² As the strength of the applied electric field increases, the average kinetic energy of the free electrons is sufficient to ionize neutral centers. The recombination process is less effective at high fields since the capture cross section decreases with increasing carrier energy. At electric field intensities exceeding a certain

critical value the ionization rate is greater than the rate of recombination, and a nonequilibrium state is obtained. The critical field for breakdown is expressed in terms of the kinetic equation¹³

$$\frac{dn}{dt} = A_T(N_D - N_A - n) + nA_I(N_D - N_A - n) - B_T(N_A + n) - n^2B_I(N_A + n), \quad (6)$$

where A_T , A_I represent rates of carrier generation by thermal and impact ionization, and B_T , B_I are the thermal and Auger recombination rates, respectively. Under steady-state conditions, if we neglect the Auger recombination and thermal generation and assume that both $N_D - N_A$, $N_D \gg n$, we have

$$A_I(N_D - N_A) = B_T N_A \quad (7)$$

as a simple expression for the breakdown condition.

The impact-ionization and thermal-recombination coefficients are dependent on a number of parameters including lattice temperature and the carrier distribution. The impact-ionization coefficient A_I for a trap with depth \mathcal{E}_i can be computed from a recent treatment by Cohen and Landsberg.¹⁰

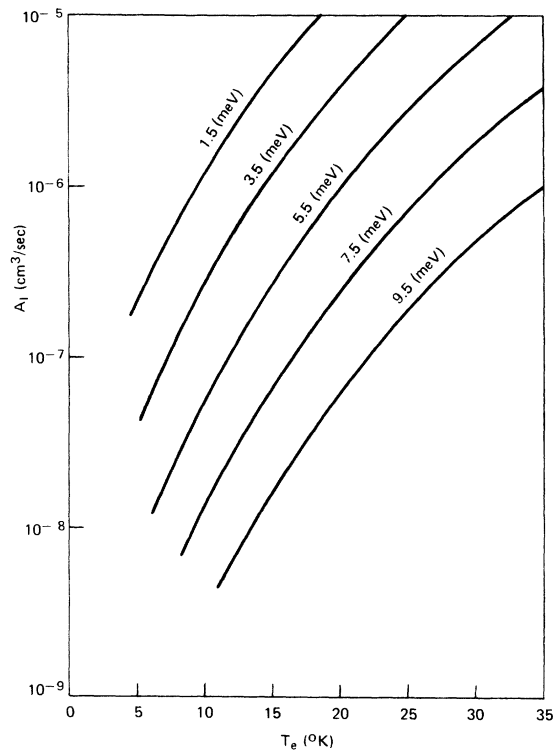


FIG. 8. Impact-ionization coefficient as a function of electron temperature for different impurity level depths (indicated).

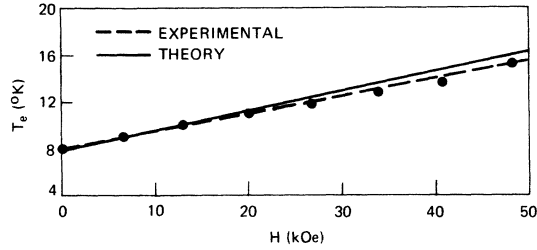


FIG. 9. Electron temperature required for breakdown in *n*-type GaAs as a function of magnetic field.

The results of such a calculation showing the ionization coefficient as a function of electron temperature for various impurity ionization energies is shown in Fig. 8. The electron temperature may be related to the breakdown electric field by the semiempirical relation¹⁰

$$T_e(^{\circ}\text{K}) = A[(\mu_F/\mu_0)E_B]^{1/2}, \quad (8)$$

where the parameter A for samples of impurity concentration of this paper is approximately $3.5^{\circ}\text{K}(\text{cm}/\text{V})^{1/2}$. The ratio μ_F/μ_0 (of electron mobilities with and without a magnetic field) is included to account for the reduction in mobility in a magnetic field. The thermal recombination of free carriers with a trapping center can be calculated by assuming the carriers are captured by highly excited trapping states.¹⁴ The carrier loses energy by emission of a series of phonons as the carrier cascades down through the series of excited states of the center. The thermal-recombination coefficient can approximately be described by the relation⁹

$$B_T = 1.0 \times 10^{-5}/T_e \text{ cm}^3/\text{sec}, \quad (9)$$

where T_e is the electron temperature and the numerical coefficient has been derived from approximate theories^{9,10} and a similar treatment of impurities in germanium.¹⁵

From Fig. 6 it is apparent that as the impurity ionization energy increases as a result of an applied magnetic field, higher electron temperatures are required to reach ionization rates satisfying the breakdown condition [Eq. (7)]. The increase in electron temperature is achieved by stronger elec-

tric fields according to Eq. (8) which takes into account the effect of the magnetic field on the rate at which carriers are heated through the mobility ratio μ_F/μ_0 . From this electric field strength and carrier temperature we can drive the experimental electron temperature at breakdown as a function of magnetic field strength (Fig. 9). The electron temperature required for ionization can be calculated theoretically by combining the breakdown relation [Eq. (7)] and the expression for B_T [Eq. (9)], giving

$$A_I = (1 \times 10^{-5})N_A/(N_D - N_A)T_e = 2 \times 10^{-6}/T_e \quad (10)$$

using a compensation ratio of 0.2. Using this relation and Fig. 7 which uniquely relates A_I and T_e for an impurity level of a known ionization energy, we may determine an electron temperature required for breakdown. These values are compared with the experimental values in Fig. 9 with the data of Fig. 6 being used to relate impurity ionization energy to magnetic field strength. Agreement between the experimental and calculated results is reasonably good, and shows an increase in electron temperature for breakdown from 8 to 16 °K as the magnetic field is increased to approximately 50 kOe.

CONCLUSION

The experiments reported here in strongly doped *n*-type GaAs show that the low-temperature impurity phenomena is properly described using density-of-states functions for the conduction band and impurity level which have Gaussian-like tails. Both magnetic freezeout and impurity ionization experiments appear to be in agreement in this recently developed model for strongly doped semiconductors in a magnetic field. A proper interpretation of measurements on impurity activation energy and impact ionization leads to the conclusion that states deep in the conduction-band tail are sufficiently localized that they do not contribute to the conduction process. Changes in the electric breakdown fields of these materials in a magnetic field appear to be in agreement with recent theories of impact ionization provided the increase in activation in a magnetic field is properly taken into account.

†Work supported by the Department of the Navy under Contract No. N00017-62-c-0604.

¹J. Whitaker and D. E. Bolger, *Solid State Commun.* **4**, 181 (1966).

²R. Kaplan, M. A. Kinch, and W. C. Scott, *Solid State Commun.* **7**, 883 (1969).

³J. M. Chamberlain and R. A. Stradling, *Solid State Commun.* **7**, 1275 (1969).

⁴O. Beckman, E. Hanamura, and L. J. Neuringer, *Phys. Rev. Letters* **18**, 773 (1967).

⁵L. A. Kaufman and L. J. Neuringer, *Phys. Rev. B*

2, 1840 (1970).

⁶Y. Yafet, R. W. Keyers, and E. N. Adams, *J. Phys. Chem. Solids* **1**, 137 (1956).

⁷D. M. Larsen, *J. Phys. Chem. Solids* **29**, 271 (1968).

⁸M. I. Dyakonov, A. L. Efros, and D. L. Mitchell, *Phys. Rev.* **180**, 813 (1969).

⁹J. Yamashita, *J. Phys. Soc. Japan* **16**, 720 (1961).

¹⁰M. E. Cohen and P. T. Landsberg, *Phys. Rev.* **154**, 683 (1967).

¹¹N. F. Mott, *Phil. Mag.* **19**, 835 (1969).

¹²S. H. Koenig, R. D. Brown, and W. Schillinger,

Phys. Rev. 128, 1668 (1962).

¹³S. H. Koenig, Phys. Rev. 110, 986 (1958).

¹⁴M. Lax, J. Phys. Chem. Solids 8, 66 (1959).

¹⁵T. O. Poehler and J. R. Apel, Phys. Rev. B 1, 3240 (1970).

PHYSICAL REVIEW B

VOLUME 4, NUMBER 4

15 AUGUST 1971

Excited Impurity States and Transient Photoconductivity in Cobalt-Doped Silicon[†]

M. C. P. Chang and Claude M. Penchina

*Department of Physics and Astronomy, University of Massachusetts,
Amherst, Massachusetts 01002*

and

J. S. Moore*

*Department of Electrical Engineering and Center for Materials Science and Engineering,
Massachusetts Institute of Technology, Cambridge, Massachusetts 02139*

(Received 10 February 1971)

We have studied extrinsic optical absorption and transient photoconductivity due to the two deep impurity levels that cobalt introduces in silicon. The absorption and photoconductivity spectra show that the acceptor level 0.52 eV below the conduction-band edge and the donor level 0.38 eV above the valence-band edge are two different charge states of the same cobalt center, rather than independent states. The long-wavelength optical absorption spectra and the transient response times of positive and negative photoconductivity can be explained in terms of various excited states of neutral, and of positively charged cobalt centers. These excited states lead to a modification in the kinetics of the previously proposed two-level model of negative photoconductivity.

I. INTRODUCTION

Cobalt in silicon has previously been found to introduce deep impurity levels which cause light-sensitive oscillatory current instabilities.^{1,2} Studies of the effects of infrared light on the oscillations led us to the discovery of negative extrinsic photoconductivity³ in *n*-type Co-compensated Si, which was interpreted by a previously proposed model.^{3,4} However, the photosignal was sufficiently weak and the samples sufficiently thin that we were unable to observe either the transient response of photoconductivity or the extrinsic optical absorption under monochromatic illumination. Recently,⁵ experiments on diffusion of Co in Si have demonstrated the ability of Co to compensate *p*-type Si and have located the Co impurity levels more accurately. They were found to be a donor 0.38 ± 0.02 eV from the valence band and an acceptor 0.52 ± 0.02 eV from the conduction band.

We report here on more thorough and extensive investigations of the optical properties of this material. Larger samples made possible the study of the extrinsic optical-absorption spectrum, and a signal-averaging computer made possible a study of the spectral response of transient photoconductivity. These optical data confirm the location of the levels as mentioned above⁵ and indicate that they are two different charge states of the same

center. Also, from photoconductivity measurements, we have evidence of free-carrier capture on excited centers.

II. MEASUREMENTS

Absorption measurements in the 1.1–2.6- μ region were done on a Cary model 14 double monochromator. For longer wavelengths, a Beckman model IR-10 was used.

For photoconductivity measurements, a Spex $\frac{3}{4}$ -m grating monochromator was used to illuminate the sample with extrinsic light chopped by a piezoelectric chopper with variable chopping rate. Photoconductivity transient response signals were processed with a computer of average transients (TMC CAT 4606) to increase the signal-to-noise ratio.

III. SAMPLE PREPARATION

Silicon wafers were prepared for diffusion by degreasing in hot trichloroethane, etching in HF + HNO₃, rinsing in HNO₃, and then rinsing in distilled deionized water. They were then chelated in the trisodium salt of ethylenediamine tetracetic acid (EDTA), rinsed again in deionized water, and dried on filter paper. At least an order of magnitude more cobalt than necessary to compensate to the solid solubility limit⁶ of 10^{16} cm⁻³ was quickly evaporated on both faces of the wafer, and the cobalt-plated silicon was then sealed in an argon-

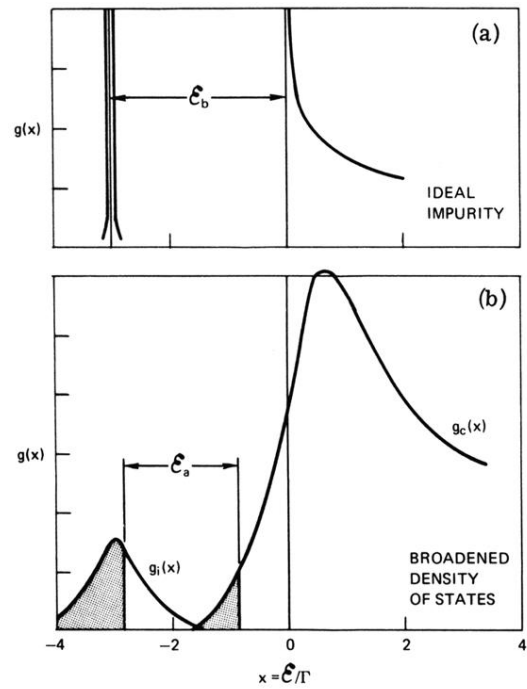


FIG. 5. Density-of-states functions for n -type GaAs in a strong magnetic field. (a) Ideal case of lightly doped specimen with binding energy \mathcal{E}_b . (b) Broadened density-of-states functions in strongly doped material with ionization energy \mathcal{E}_i . Energy normalized by Γ , where $\Gamma \cong 3$ meV at $H=40$ kOe.